Journal of Advanced Ceramics
2012, 1(2): 150-156
DOI: 10.1007/s40145-012-0013-1 ISSN 2226-4108

Research Article

Effect of transition metal oxides doping on $Ce_{0.9}Sm_{0.05}Nd_{0.05}O_{1.95}$ solid electrolyte materials

Ming ZHOU, Lin GE, Han CHEN, Lucun GUO*

College of Materials Science and Engineering, Nanjing University of Technology, No.5 Xinmofan Road, Nanjing, 210009, China

Received August 26, 2011; Accepted December 14, 2011

Abstract: The effect of transition metal oxides (TMOs) $CoO_{1.5}$, $FeO_{1.5}$ and MnO_2 addition on $Ce_{0.9}Sm_{0.05}Nd_{0.05}O_{1.95}$ was studied. The crystal structures, microstructures, thermal expansion and electrical properties were characterized by X-ray diffraction (XRD), scanning electron microscopy (SEM), dilatometer and AC impedance spectroscopy，respectively. The results show that the TMOs addition remarkably promotes the densification of $Ce_{0.9}Sm_{0.05}Nd_{0.05}O_{1.95}$ and reduces the sintering temperature by ~150 ℃. The samples with TMOs addition sintered at 1450 ℃ exhibit higher conductivities than those sintered at 1500 ℃. The maximum conductivity of 0.040 $s.cm^{-1}$ at 700 ℃ was achieved with 1 mol% $FeO_{1.5}$ doping when sintered at 1450 ℃. In addition, the thermal expansion was linear for all the samples. The doping of TMOs does not appreciably change thermal expansion coefficient.

Key words: transition metal oxides; microstructure; thermal expansion; ionic conductivity

1 Introduction

In recent years, solid oxide fuel cells (SOFCs) are of considerable interest as a promising energy conversion device due to their advantages such as high efficiency, low emission of pollutants and a wide variety of available fuels [1,2].

Solid electrolytes are the most important and indispensable component of SOFCs that govern the performance and to a large extent the design of the system [3]. Currently, the yttria-stabilized zirconia (YSZ) is the commonly applied electrolyte for SOFCs, however, its high operating temperature (800-1000 ℃) leads to a severe criteria for other construction materials, as well as short service times [4,5]. Therefore, intensive research has focused on new, improved oxide-ion electrolytes at intermediate temperature (IT) range (300-700 ℃) [6].

Doped-CeO_2 has emerged as potential electrolyte materials for IT-SOFCs because of their high conductivity and good compatibility with electrodes [7,8]. In the family of doped ceria electrolytes, numerous studies have been conducted to investigate the relationship between ionic conductivity and dopant. It is reported that Nd^{3+} and Sm^{3+} co-doped may result in the enhancement of ionic conductivity. Both Li et al and Omar et al group found that Sm^{3+} and Nd^{3+}

* Corresponding author.
E-mail: lc-guo@163.com

co-doped $Ce_{0.9}Sm_{0.05}$ $Nd_{0.05}O_{1.95}$ (SNDC) exhibited excellent ionic conductivity in IT-range [3,9,10]. Nevertheless, as a result of the refractory nature, the SNDC electrolyte material should be sintered around 1600 ℃ to obtain proper apparent density. Such a high temperature will cause atomic diffusion and solid reactions between cell components during the fabrication process, which has a detrimental effect on the performance of SOFCs [4,11]. To overcome this problem, addition of sintering aids to promote densification has been adopted. Many sintering aids such as MnO_2, Fe_2O_3 and Co_2O_3 were used in CeO_2-based electrolytes and have been proved to be effective [12-15].

In this paper, 1 mol% transition metal M (M=Fe, Co and Mn) were added to $Ce_{0.9}Sm_{0.05}Nd_{0.05}O_{1.95}$ in the form of metal oxide, the aim was to improve the sinterability of SNDC. The effect of transition metal doping on thermal expansion and ionic conductivity was also investigated and discussed.

2 Experiment

2.1 Preparation

A series of samples with the general formula $Ce_{0.9}Sm_{0.05}Nd_{0.05}O_{1.95}$, $(Ce_{0.9}Sm_{0.05}Nd_{0.05}O_{1.95})_{0.99}(CoO_{1.5})_{0.01}$, $(Ce_{0.9}Sm_{0.05}Nd_{0.05}O_{1.95})_{0.99}(FeO_{1.5})_{0.01}$ and $(Ce_{0.9}Sm_{0.05}Nd_{0.05}O_{1.95})_{0.99}(MnO_2)_{0.01}$ (noted as SNDC , SNDC-Co1, SNDC-Fe1 and SNDC-Mn1) were prepared by solid state reaction method using CeO_2 (99.99%, in mass, the same below), Sm_2O_3 (99.99%), Nd_2O_3 (99.99%), Fe_2O_3(99.99%), Co_2O_3(99.99%) and MnO_2(99.99%) as starting materials. The raw materials were weighted according to the stochiometric ratio and dissolved in deionized water. The mixed powders were then ball milled for 8 h using zirconia (ZrO_2) as milling media The powders were dried and then grounded and calcined at 1200 ℃ in air for 2 h. After calcination, the as-synthesized powders were ball milled again for 6 h and dried. The dried powders were ground in an agate mortar and die-pressed under a pressure of about 85 MPa into cylindrical pellets (27 mm in diameter and 1 mm in thickness). The green pellets with TMOs addition were sintered at 1450-1500 ℃ for 2 h, while the undoped SNDC was sintered at 1600 ℃ for 5 h for comparison. Bars of 62 mm×5 mm×5 mm were also pressed at 100 MPa to investigate the thermal expansion behavior.

2.2 Characterization

The densities of the sintered pellets were determined by the Archimedean method. Their crystal structures were identified via X-ray diffraction (XRD, D/maxIII Rigaku) with Cu K_α radiation at room temperature in the Bragg angle range from 20° to 80°. Surfaces of the samples were examined by JSM-5900 (JEOL, Japan) scanning electron microscope (SEM). Thermal expansion was measured in air using a dilatometer (RPZ-01, Luoyang Refractory Material Researching Company, China) from room temperature to 700 ℃ with a heating rate of 5 ℃/min.

For ionic conductivity measurement, silver paste was painted onto both sides of the pellets and the samples were baked at 700 ℃ for 10 min. The impedance complex spectra of the pellets were measured using a Parstat 2273 frequency response analyzer (Ametek, US). The measurement was conducted in air from 300 ℃ to 700 ℃ at an interval of 50 ℃ and in the frequency range from 0.1 Hz to 0.1 MHz. An excitation of 50 mV was applied at all the test temperatures. The curve fitting and resistance calculation were carried out using ZSimpWin software.

3 Results and discussion

3.1 Sinterability and microstructure

Figure 1 shows the relative densities of the samples at different temperatures. The TMOs-doped samples all achieve high relative densities of more than 94% at 1450 ℃ and 1500 ℃ while it is only 74.9% (at 1450 ℃) and 88.4% (at 1500 ℃) for undoped SNDC. The SNDC must be sintered at 1600 ℃ for 5 h to obtain 98% relative density. The SEM photographs of the samples sintered at 1450 ℃ are presented in Figs. 2a-2d. As can be seen, the sample without TMO doping is found to be very porous. In contrast, all the samples with TMOs addition are well dense. It is inferred that the TMOs doping has a significant effect on the densification process of SNDC, the rapid densification of TMO-added samples may be attributed to a liquid-phase sintering mechanism: the presence of a liquid formed by the TMOs leaded to an increased area of contract among the particles during the sintering process. This in turn promoted the mass diffusivity and consequently the sinterability, as indicated by previous studies [2,16,17].

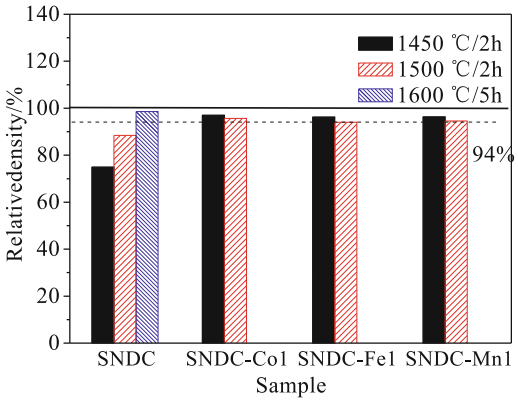

Fig. 1 Relative densities of the samples at different temperatures

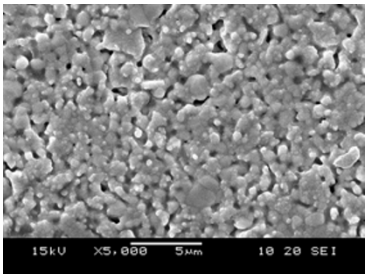

(a) SNDC

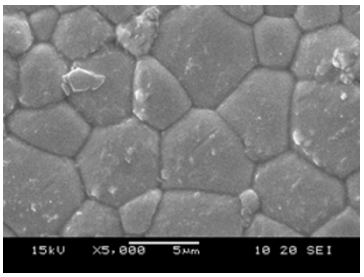

(b) SNDC-Co1

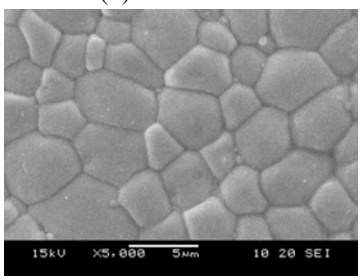

(c) SNDC-Fe1

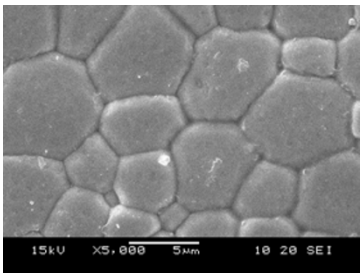

(d) SNDC-Mn1

Fig. 2 SEM photographs of samples sintered at 1450 ℃ for 2 h

3.2 Crystal structure

Figure 3 shows the XRD patterns of TMO-doped SNDC sintered at 1450 ℃ for 2 h. The undoped SNDC sintered at 1600 ℃ for 5 h is also shown for comparison. Only a single phase of ceria with Fm3m cubic fluorite is identified for all the samples. It is indicated that the crystal structure of SNDC is not altered with the addition of TMOs. This implies that the TMOs are present at concentrations below the XRD limit.

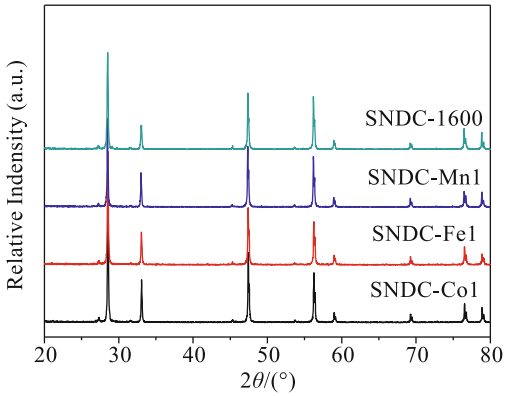

Fig. 3 XRD patterns of SNDC with TMOs doping

3.3 Ionic conductivity

The ionic conductivities of samples were measured by means of two probe AC impedance spectroscopy. Generally, the impedance spectroscopy consists of several independent semicircular arcs from high frequency to low frequency which reflect conduction across the grain interior (GI), grain boundary (GB) and electrode-electrolyte. Fig. 4a shows the impedance spectra of TMO-doped samples sintered at 1450 ℃ for 2 h, the undoped SNDC sintered at 1600 ℃ for 5 h is also included. The testing temperature is 300 ℃. As can be seen from Fig. 4a, the impedance spectroscopy consists of two arcs which can be attributed to the contributions of GB and electrode interfaces. Unfortunately, the arc in high frequency which reflects the conduction process occurring in the bulk is not presented because of the limited frequency of testing equipment (0.1 Hz to 0.1 MHz). Figure 4b presents the equivalent circuit model used to fit the impedance spectra. The equivalent circuit model includes a series of parallel resistances R and capacitances C. Considering the inhomogeneity of microstructure within the sintered sample, the capacitance C was substituted by constant phase element (CPE). The total

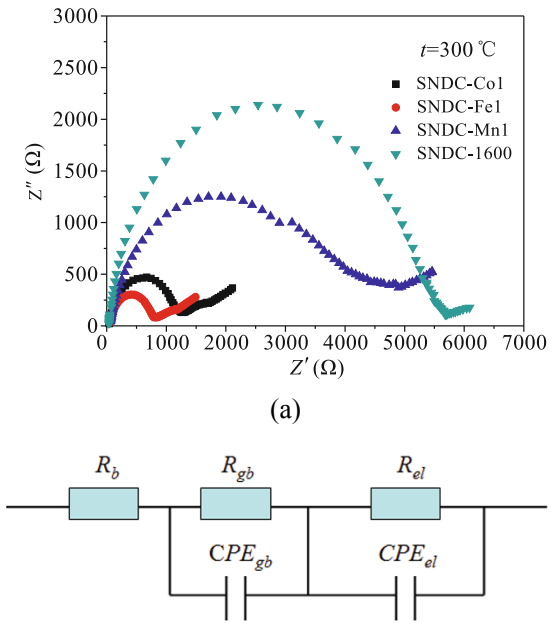

Fig. 4 Impedance spectra of samples sintered at 1450 ℃ and equivalent circuit model used to fit the impedance spectra. (a) Impedance spectroscopy of samples at 300 ℃. (b) Equivalent circuit model used to fit the impedance spectra

resistance is given by

$$R = R_b + R_{gb} \quad (1)$$

where R_b and R_{gb} stand for the resistance of GI and GB respectively and can be both obtained by fitting the impedance data. Then the ionic conductivity σ can be calculated according to the equation

$$\sigma = \frac{L}{SR} \quad (2)$$

where L is the thickness of sample and S is the area of electrode.

Through fitting the data and using the Eqs. (1) and (2), the ionic conductivities of samples at different temperatures can be obtained. Table 1 lists the total (σ_t), GI (σ_{gi}) and GB (σ_{gb}) conductivities of SNDC ceramics with TMOs sintered at 1450 ℃. The dense SNDC sintered at 1600 ℃ (notes as SNDC-1600) is also presented for comparison. The testing temperature is 300 ℃.

Table 1 Total (σ_t), GI (σ_{gi}) and GB (σ_{gb}) conductivities of each sample sintered at 1450 ℃

Sample	σ_{gi} (s·cm^{-1})	σ_{gb} (s·cm^{-1})	σ_t (s·cm^{-1})
SNDC-Co1	2.29×10^{-3}	5.13×10^{-5}	5.02×10^{-5}
SNDC-Fe1	2.15×10^{-3}	1.24×10^{-4}	1.14×10^{-4}
SNDC-Mn1	1.84×10^{-3}	2.52×10^{-5}	2.48×10^{-5}
SNDC-1600	1.67×10^{-3}	1.29×10^{-5}	1.28×10^{-5}

Note: Testing temperature is 300 ℃.

It is noted that the TMOs addition increases the GI conductivity of SNDC slightly, while it has a significant effect on GB conductivity. The remarkable improvement of GB conductivity by TMOs addition maybe due to the formation of a TMO-rich grain boundary layer: the TMO ions easily located at the grain boundaries during the sintering process and resulted in different distortions of the surrounding lattices and higher oxygen vacancy mobility through the grain boundaries, thus improved the GB conductivity [5,11]. The SNDC-Fe1 has the maximum GB conductivity, it is reported that compared with MnO_2 and $CoO_{1.5}$, $FeO_{1.5}$ can not only alter the oxygen vacancy mobility in the grain boundary as discussed above, it also acted as a scavenger by reacting with SiO_2 in the grain boundary which further decreased the resistance of grain boundary [18]. Therefore, it can be concluded that $FeO_{1.5}$ can improve the conductivity of SNDC more significantly than those of $CoO_{1.5}$ and MnO_2.

The total ionic conductivities of TMOs-doped SNDC sintered at 1450 ℃ for 2 h (SNDC sintered at 1600 ℃) was presented in Fig. 5 in the form of $\ln(\sigma T)$ versus $10^4/T$.

It can be seen that the TMOs-doped samples all exhibit higher total conductivities than undoped SNDC, which is mainly attributed to the improvement of GB conductivity as presented above. Among the testing samples, SNDC-Fe1 exhibits the highest conductivity of 0.040 s·cm^{-1} at 700 ℃. In addition, the well linear relationship between $\ln(\sigma T)$ and $10^4/T$ in Fig. 5

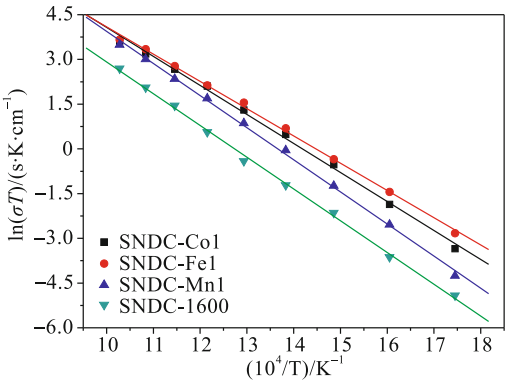

Fig. 5 Total conductivities of TMO-doped samples sintered at 1450 ℃ for 2 h

suggests that all the data obey the Arrhenius equation:

$$\sigma = \frac{A}{T}\exp\left(-\frac{E_a}{kT}\right) \quad (3)$$

where σ is conductivity, E_a is the activation energy for ionic migration, k is the Boltzman's constant, T is the absolute temperature and A is the pre-exponential factor being a constant in certain temperature range.

Table 2 presents the total (σ_t), GI (σ_{gi}) and GB (σ_{gb}) conductivities of SNDC ceramics with TMOs sintered at 1500 ℃. Similar to Table 1, the improvement of total ionic conductivity with TMOs addition is mainly due to the increase of GB conductivity as discussed above. However, the TMOs-doped samples sintered at 1500 ℃ all exhibit lower GB conductivities than those sintered at 1450 ℃. As proposed by Guo and Waser [19], there exists a space charge layer which results in the depletion of oxygen vacancies near the GB, the increase of temperature leads to the well developed space charge layer in the GB which aggravates the depletion of oxygen vacancies in the vicinity of GB and thus decreases the GB conductivity.

Figure 6 presents the total ionic conductivities of TMO-doped samples sintered at 1500 ℃ for 2 h. It can be seen that the TMO-doped samples exhibit higher conductivities than undoped SNDC which is similar to Fig. 5 and SNDC-Fe1 has the maximum conductivity of 0.036 s·cm^{-1} at 700 ℃.

Table 2 Total (σ_t), GI (σ_{gi}) and GB (σ_{gb}) conductivities of each sample sintered at 1500 ℃

Sample	σ_{gi} (s·cm^{-1})	σ_{gb} (s·cm^{-1})	σ_t (s·cm^{-1})
SNDC-Co1	2.00×10^{-3}	2.69×10^{-5}	2.65×10^{-5}
SNDC-Fe1	2.62×10^{-3}	6.10×10^{-5}	5.96×10^{-5}
SNDC-Mn1	2.31×10^{-3}	1.53×10^{-5}	1.52×10^{-5}
SNDC-1600	1.67×10^{-3}	1.29×10^{-5}	1.28×10^{-5}

Note: Testing temperature is 300 ℃.

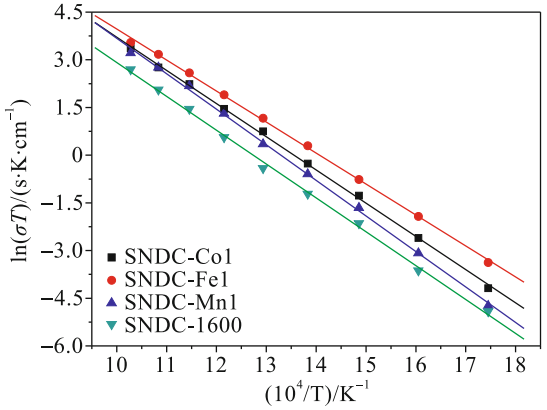

Fig. 6 Total conductivities of TMOs-doped samples sintered at 1500 ℃ for 2 h

The activation energies of the samples calculated at different temperatures are shown in Fig. 7. It is shown that the values of activation energy at 1450 ℃ are lower than those at 1500 ℃. In comparison with SNDC sintered at 1600 ℃, SNDC-Co1 and SNDC-Fe1 both show lower values of activation energy while SNDC-Mn1 has slight higher activation energy at different temperatures. The SNDC-Fe1 has the minimum energy of 0.787 eV at 1450 ℃ and 0.840 eV at 1500 ℃.

3.4 TEC measurements

The thermal expansion behavior of TMO-doped SNDC sintered at 1450 ℃ for 2 h (SNDC sintered at 1600 ℃ for 5 h) from 100 ℃ to 700 ℃ is shown in Fig. 8. It can be seen that all the samples exhibit linear temperature dependence. The thermal expansion coefficients (TECs) of samples calculated are listed in Table 3. As shown in Table 3, the TECs of all the

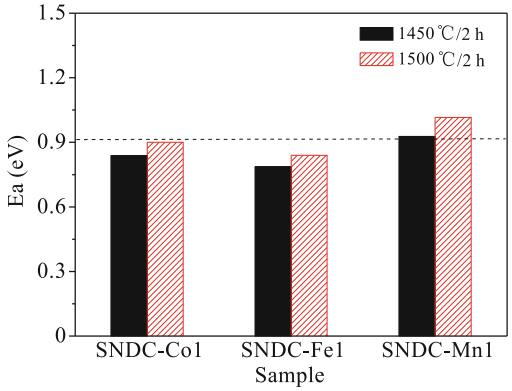

Fig. 7 Activation energies of the TMOs-doped samples at different temperatures

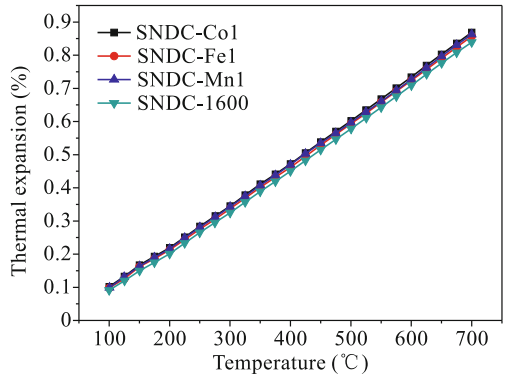

Fig. 8 Linear thermal expansion curves for sample with different TMOs doping

Table 3 Thermal expansion coefficients of each sample

Sample	TEC×10^{-6} (K^{-1})
SNDC-Co1	12.28
SNDC-Fe1	12.07
SNDC-Mn1	12.16
SNDC-1600	12.83

tested samples are in accordance with the typical TEC values of CeO_2-based materials. The addition of TMO slightly decreases the TEC of SNDC and the smallest TEC value of $12.07\times10^{-6}K^{-1}$ is obtained for SNDC-Fe1.

4 Conclusions

The TMOs such as $CoO_{1.5}$, $FeO_{1.5}$ and MnO_2 were added to SNDC as a sintering aid and can be able to reduce the sintering temperature of solid electrolyte ceramic SNDC by ~150 ℃. The samples with TMOs addition sintered at 1450 ℃ showed higher conductivities than those sintered at 1500 ℃. Among the testing samples, the SNDC-Fe1 sintered at 1450 ℃ exhibited the maximum conductivity which reached 0.040 $s.cm^{-1}$ at 700 ℃ and it was a promising candidate as the electrolyte material for IT-SOFCs.

Acknowledgement

We acknowledge support of Jiangsu Provincial Key Laboratory of Inorganic and Composite Materials.

References

[1] Li SJ, Ge L, Gu HH, *et al*. Sinterability and electrical properties of ZnO-doped $Ce_{0.8}Y_{0.2}O_{1.9}$ electrolytes prepared by an EDTA-citrate complexing method. *J Alloys Compd* 2011, **509**: 94-98.

[2] Wang ZW, Hashimoto SI, Mori M. Investigation and optimization of interface reactivity between $Ce_{0.9}Gd_{0.1}O_{1.95}$ and $Zr_{0.89}Sc_{0.1}Ce_{0.01}O_{2-\delta}$ for high performance intermediate temperature-solid oxide fuel cells. *J Power Sources* 2009, **93**: 49-54.

[3] Omar S, Wachsman ED, Jones JL, *et al*. Crystal structure-Ionic conductivity relationships in doped ceria systems. *J Am Ceram Soc* 2009, **11**: 2674-2681.

[4] Gao L, Zhou M, Zheng YF, *et al*. Effect of zinc oxide on yttria doped ceria. *J Power Sources* 2010, **195**: 3130-3134.

[5] Li B, Wei X, Pan W. Electrical properties of Mg-doped $Gd_{0.1}Ce_{0.9}O_{1.95}$ under different sintering temperature. *J Power Sources* 2008, **183**: 498-505.

[6] Fu YP, Chen SH, Huang JJ. Preparation and characterization of $Ce_{0.8}M_{0.2}O_{2-\delta}$ (M=Y, Gd, Sm, Nd, La) solid electrolyte materials for solid oxide fuel cells. *Int J Hydrog Energy* 2010, **35**: 745-752.

[7] Ahn JS, Omar S, Yoon HS, *et al*. Performance of anode-supported solid oxide fuel cell using novel ceria electrolyte. *J Power Sources* 2010, **195**: 2131-3135.

[8] Dikmen S, Aslanbay H, Dikmen E, *et al*. Preparation and electrochemical properties of Gd^{3+} and Bi^{3+}, Sm^{3+}, La^{3+}, and Nd^{3+}codped ceria-based electrolytes for intermediate temperature-solid oxide fuel cell. *J Power Sources* 2010, **195**: 2488-2495.

[9] Li B, Liu YY, Wei X, *et al*. Electrical properties of ceria Co-doped with Sm^{3+} and Nd^{3+}. *J Power Sources* 2010, **195**: 969-976.

[10] Li B, Wei X, Pan W. Improved electrical conductivity of $Ce_{0.9}Gd_{0.1}O_{1.95}$ and $Ce_{0.9}Sm_{0.1}O_{1.95}$ by co-doping. *Int J Hydrog Energy* 2010, **35**: 3018-3022.

[11] Ayawanna J, Wattanasiriwech D, Wattanasiriwech S, *et al*. Effects of cobalt metal addition on sintering and ionic conductivity of Sm(Y)-doped ceria solid electrolyte for SOFC. *Solid State Ion* 2009, **180**: 1388-1394.

[12] Dutta A, Kumar A, Basu RN. Enhanced electrical conductivity in $Ce_{0.79}Gd_{0.20}Co_{0.01}O_{2-\delta}$ for low temperature solid oxide fuel cell applications. *Electrochem Commun* 2009, **11**: 699-701.

[13] Foschini CR, Souza DPF, Filho PIP, *et al*. AC impedance study of Ni, Fe, Cu, Mn doped ceria stabilized zirconia ceramics. *J Eur Ceram Soc* 2001, **21**: 1143-1150.

[14] Zhang TS, Hing P, Huang HT, *et al*. The effect of Fe doping on the sintering behavior of commercial CeO_2 powder. *J Mater Process Technol* 2001, **113**: 463-468.

[15] Lewis GS, Atkinson A, Steele BCH, *et al*. Effect of Co addition on the lattice parameter, electrical conductivity and sintering of gadolinia-doped ceria. *Solid State Ion* 2002, **152-153**: 567-573.

[16] Kondakindi RR, Karan K. Characterization of Fe- and Mn-doped GDC for low-temperature processing

of solid oxide fuel cells. *Mater Chem Phys* 2009, **115**: 728-734.

[17] Zhang TS, Ma J, Leng YJ, *et al*. Effect of transition metal oxides on densification and electrical properties of Si-containing $Ce_{0.8}Gd_{0.2}O_{2-\delta}$ ceramics. *Solid State Ion* 2004, **168**: 187-195.

[18] Zhang TS, Ma J, Leng YJ, *et al*. Iron oxide as an effective sintering aid and a grain boundary scavenger for ceria-based electrolytes. *Solid State Ion* 2004, **167**: 203-207.

[19] Guo X, Waser R. Electrical properties of the grain boundaries of oxygen ion conductors: Acceptor-doped zirconia and ceria. *Prog Mater Sci* 2006, **51**: 151-210.